Available online at www.sciencedirect.com
ScienceDirect
Journal of Sound and Vibration 300 (2007) 490–501
JOURNAL OF SOUND AND VIBRATION
www.elsevier.com/locate/jsvi

Stochastic road excitation and control feasibility in a 2D linear tyre model

E. Rustighi*, S.J. Elliott

Institute of Sound and Vibration Research, Southampton, UK

Received 14 November 2005; received in revised form 26 May 2006; accepted 1 June 2006
Available online 30 October 2006

Abstract

For vehicle under normal driving conditions and speeds above 30–40 km/h the dominating internal and external noise source is the sound generated by the interaction between the tyre and the road. This paper presents a simple model to predict tyre behaviour in the frequency range up to 400 Hz, where the dominant vibration is two dimensional. The tyre is modelled as an elemental system, which permits the analysis of the low-frequency tyre response when excited by distributed stochastic displacements in the contact patch. A linear model has been used to calculate the contact forces from the road roughness and thus calculate the average spectral properties of the resulting radial velocity of the tyre in one step from the spectral properties of the road roughness. Such a model has also been used to provide an estimate of the potential effect of various active control strategies for reducing the tyre vibrations.

1. Introduction

Nowadays, because of the development of more silent vehicle power units, the main source of internal and external car noise is the interaction between the tyre and road. For a vehicle at normal driving conditions and speeds above 30–40 km/h the dominating external noise source is the sound generated by the tyre and road interaction [1]. Measurements on the noise generation mechanism show that there is a strong correlation between the radiated sound pressure and the vibrations of the tyre structure for frequencies below approximately 1 kHz [2]. Moreover, the recent design of lightweight vehicles has increased the significance of the road/tyre noise inside the vehicle due to structure-born vibration and acoustic radiation, affecting the passenger comfort [3].

Various models have been used to predict the noise generated by the interaction between a rolling tyre and the road surface [4]. These models can be classified in three categories: empirical models [2], deterministic models [5] and hybrids models [6]. While deterministic models try to model the physical processes involved, empirical models try to find relationship among experimental measured data. Hybrid models apply deterministic model in order to represent the contact nonlinearity and rely on empirical analysis in order to find data correlations.

*Corresponding author.
E-mail addresses: er@isvr.soton.ac.uk (E. Rustighi), sje@isvr.soton.ac.uk (S.J. Elliott).

0022-460X/$ - see front matter © 2006 Elsevier Ltd. All rights reserved.
doi:10.1016/j.jsv.2006.06.076

Each of these models could be used to identify the global behaviour of the system, from road surface characteristics to noise production. Besides these, there are models that only describe a part of the full system, as for instance those that focus on tyre vibration. One of the first low-frequency tyre models was the circular ring model introduced by Böhm and described by Kropp [7]. The tyre belt was modelled as a ring on an elastic foundation that represented the sidewalls and the enclosed air in the cavity. The ring was also exposed to a tension force simulating the inflation pressure. A series of publications followed this work, improving the original model and extending its frequency range of applicability [8–10].

Road surface texture and tyre tread pattern create fluctuating forces that excite the tyre structure, producing vibrations. The interaction is made nonlinear by the time-varying nature of the contact area. Clapp [11] developed a numerical method to predict the contact pressure that results from road surface texture. His method is based on elasticity theory and a simplified two-dimensional contact model where the road is considered rigid and the tyre modelled as an half-space. Wullens and Kropp [12] developed a three-dimensional contact model for the tyre–road interaction in rolling conditions. The contact problem has been solved using an elastic half-space and assuming the road to be rigid. Such contact models have been developed in the time-domain to account for the nonlinear interaction. Hence, only deterministic road profile can be considered in such analyses. These methods are usually complicated and time consuming, even though very detailed.

In this paper, a simple linear model is presented for the random excitation of a tyre's vibration. The analysis is entirely linear in order to exploit the simple theoretical formulation of a stochastic linear analysis and to develop a method that is computationally efficient. The linear model represents a first-order approximation to the full interaction, whose validity is tested by comparing the predicted tyre response with previous measurements. Following the introduction in the second section, the excitation of the tyre, as it runs over a rough road, is modelled as a random displacement distribution with a specified spatial correlation. In the next section some simulation results are shown. For instance, the kinetic energy associated with the radial motion of the tyre is calculated. The next section considers the effect of a controllable, secondary, force distribution and preliminary simulation results are presented. Finally, some conclusions are drawn.

2. The tyre–road model

2.1. The ring model

The tyre model used in the simulation is the stationary ring model proposed by Huang and Soedel [13]. This model can be used to account for the ring modes of the tyre that dominate its response below about 400 Hz, at which the external sound radiation from the tyre and the internal sound generation are dominated by the tyre's vibration rather than aerodynamic sources. In such a model the stiffness of the sidewalls, the inflation pressure and the loss factors of sidewalls, tread and internal pressure have been taken into account. The stiffness of the sidewalls have been modelled by a massless foundation characterised by two spring constants, k_r and k_q, that are, respectively, a radial and a tangential stiffness. The dynamics of a stationary ring are expressed by the following two equations:

$$\frac{D}{a^4}(u_r''' - u_\theta'') - \frac{K}{a^2}(u_r' + u_\theta'') + \frac{P_0}{a}(u_\theta - 2u_r' - u_\theta'') + k_\theta u_\theta + \rho h \ddot{u}_\theta = q_\theta, \tag{1}$$

$$\frac{D}{a^4}(u_r'''' - u_\theta''') + \frac{K}{a^2}(u_r + u_\theta') + \frac{P_0}{a}(u_r + 2u_\theta' - u_r'') + k_r u_r + \rho h \ddot{u}_r = q_r - P_0, \tag{2}$$

where a is the radius of the tyre, h is its thickness, $D = Eh^3/12$ is the bending stiffness, $K = Eh$ is the membrane stiffness, ρ is the density, E is the Young's modulus, P_0 is the internal pressure, q_r and q_θ are the distributed radial and tangential forces and, u_r and u_θ are the radial and the tangential displacements. Derivatives with respect to the angle θ are indicated by primes whereas derivatives with respect to the time are indicated by dots. Values for the parameters of the tyre dynamics equations have been inferred from Ref. [7] and are summarised in Table 1.

Table 1
Material parameters for the ring model of the tyre

Description and dimensions	Constant	Value
Radius of the tyre (m)	a	0.33
Tyre thickness (m)	h	0.02
Tyre width (m)	b	0.11
Young's modulus (Pa)	E	4.90×10^8
Tyre density (kg/m^3)	ρ	1000
Tangential bedding coefficient (N/m^3)	k_t	8.82×10^6
Radial bedding coefficient (N/m^3)	k_r	1.09×10^6
Rubber Poisson ratio	ν	0.45
Internal pressure (Pa)	P_0	2.00×10^5
Loss factor radial stiffness	η_r	0.05
Loss factor tangential stiffness	η_t	0.05
Loss factor longitudinal waves	η_m	0.2
Loss factor bending waves	η_k	0.3
Loss factor pressure tension	η_p	0.05
Individual contact stiffness (N/m)	k_i	1.20×10^3
Number of radial segments	N_r	92
Number of modes	N_m	15
Number of contact points	N_c	31
Velocity (km/h)	V	35

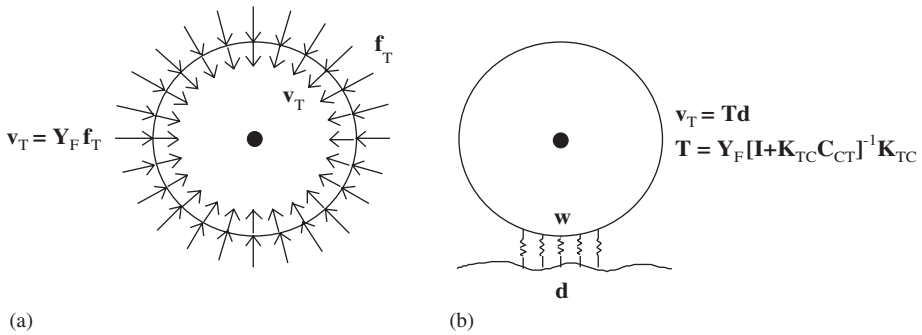

Fig. 1. Radial velocities and applied forces of the tyre suspended off the road (a). Tyre resting on the road by a Winkler bedding model of the contact (b).

Such a model does not take into account the stiffness of the suspension, nor the effects due to the rotation. Since the stiffness of the suspension has a significant effect only on the first tyre mode, as shown in Ref. [14], its influence on the tyre dynamics has been neglected at this stage. The effects of the rotation are mainly the stiffening of the tread due to the centrifugal force, which is shown to be small in Ref. [15], the Doppler shift due to the Coriolis term and the horizontal force on the hub due to the free vibration of the tread after leaving the contact patch. Although the Doppler shift will affect all the natural frequencies to same extent and could be included in a fuller treatment, it has been neglected at this stage, since the aim of this preliminary analysis was to illustrate the principle of the method, and also since most of the experimental tests that are available for comparison with the predictions from the model have been carried out on non-rotating tyres. The model also does not take into account the anti-symmetric rigid belt modes since these can only be represented by a three-dimensional model.

The tyre tread and sidewall are assumed to be divided up into N_T discrete elements, as shown in Fig. 1(a). Substituting a trial solution for the motion into Eqs. (1) and (2) for the ring dynamics, it is possible to obtain the natural frequencies and the mode shapes of the system. The mode shapes can be mass normalised and gathered in the mode shape matrix $\mathbf{\Psi}$. Once the mode shape matrix has been computed the mobility matrix

can be directly obtained. Hence, the vector of complex radial velocities at the centre of each element, $\mathbf{v}_T$, are assumed to be related to the vector of all the complex forces acting on the elements, $\mathbf{f}_T$, via the matrix of structural mobilities for the free tyre suspended off the ground, $\mathbf{Y}_F$, so that

$$\mathbf{v}_T = \mathbf{Y}_F \mathbf{f}_T. \tag{3}$$

The two-dimensional ring model can provide a good approximation to the behaviour of a real car tyre in the low-frequency range given that the parameters of the model are properly tuned to the tyre characteristics. This tuning is not always simple, however, since tyre characteristics are not generally known. In Fig. 2 the point radial mobility calculated with this ring model is compared to the mobility of a car tyre measured by Muggleton et al. [10]. The experimental data have been obtained on a treadless tyre with the hub fixed. Details of the experimental set-up and of the tyre characteristic can be found in Ref. [10]. The experimental mobility shown in Fig. 2 refers to the tyre at a pressure of 2 bar and the resonance at about 20 Hz is thought to be related to a support resonance. The parameters of the model, listed in Table 1, have been fitted to those in Ref. [10]. In general, the measured and predicted data exhibit the same overall trends, with the low frequency, stiffness-controlled region and the mid-frequency resonance groups. The measured data start to differ from the predicted ones above about 300 Hz when the high-frequency tendency towards plate-like behaviour is seen in the measurements. Furthermore, the circumferential resonances are slightly less closely spaced in the predictions than in the measured data. These observations can, in part, be attributed to the difficulty in accurately modelling the elastic properties of the tyre, which are difficult to measure and likely to be frequency dependent.

2.2. The contact model

The interaction between the tyre tread and the rough road generates a time-varying force distribution over the contact patch. It would be very convenient if a stochastic description could be developed for the tyre contact forces, using a contact model. In general, however, the contact model is rather complicated because not all of the tyre comes into contact with the road. One simplifying assumption that could be made is that the contact stiffness is generated only by a set of isolated, locally acting, springs, which is called a Winkler bedding [16]. The compression of the springs will depend on the curvature of the tyre, the road roughness and the

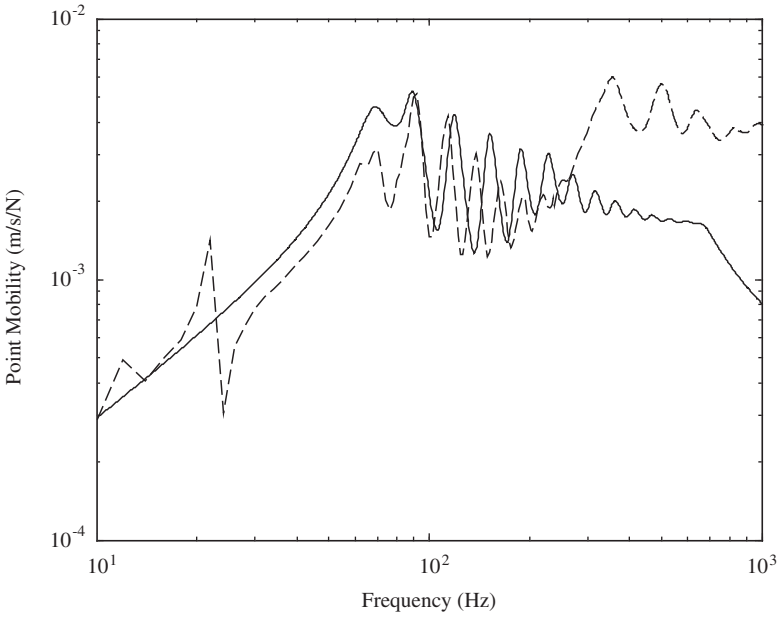

Fig. 2. Measured and predicted point mobility response: — predicted response; - - - measured response (reproduced from Ref. [10] with the permission of the authors).

vibration of the tyre belt. The tangential excitation due to friction has not been accounted for. The vibration will depend on the forces acting over the whole contact patch and this, in turn, will influence which parts of the tyre are in contact with the road and which are not. However, in this paper a very simplified contact model will be used in which it is assumed that all of the contact patch is in touch with the road at all times. The simplified linear model used here can be obtained by assuming that the tyre is smooth and soft enough that the whole of the tyre's surface in the contact patch connects with the road. In this case the spectral density matrix for the contact forces can be calculated from a statistical model of the road roughness using a linear analysis.

The tyre is assumed to be in contact with the road using such a linear contact model, which gives rise to the vector of driving forces, $\mathbf{f}_T$. In principle the distribution of forces could represent both the distribution of primary driving forces, due to road interaction in the contact patch, and a distribution of secondary forces introduced in an attempt to control the vibration of the tyre. In the simplest case, shown in Fig. 1(b), such a model consists of a Winkler bedding of N_C independent springs that connect each point on the road with vertical displacement $\mathbf{d}$ to each point in the contact patch on the tyre, with vertical tyre displacement $\mathbf{w}$, which are assumed to be equal to the radial tyre displacements since the contact patch is usually small compared with the circumference.

The force at all N_T points on the tyre is related to the difference between the road and tyre displacements by the linear equation

$$\mathbf{f}_T = \mathbf{K}_{TC}(\mathbf{d} - \mathbf{w}), \tag{4}$$

where $\mathbf{d}$ and $\mathbf{w}$ are $N_C \times 1$ vectors of the vertical displacement of the road and tyre in the contact patch and $\mathbf{K}_{TC}$ is an $N_T \times N_C$ matrix describing the linear contact stiffness. In the case of a Winkler bedding, $\mathbf{K}_{TC}$ has N_C elements equal to the individual contact stiffnesses k_i on the diagonal, and the other elements are zero. The value adopted for k_i is reported in Table 1. Its value has been found by assuming a value of the bending stiffness, as defined in Ref. [16], of 10^5 Pa. It is difficult to define the stiffness of the individual spring in order to give a realistic description of the elastic properties of the tread surface, and moreover, the contact stiffness depends on the specific tyre being modelled and the roughness of the road surface [17]. However, this assumed value for k_i gives a global contact stiffness of the same order of magnitude of that used in previous work [17]. Additionally, as it will be shown below, the overall model gives reasonable predictions of tread velocity and force transmission. If these properties were to be compared with the results of experiments as a specific tyre, the value k_i could be further tuned using this experimental data, as in Ref. [17].

The displacement of the tyre in the contact patch caused by these forces is now written as

$$\mathbf{w} = \mathbf{C}_{CT}\mathbf{f}_T, \tag{5}$$

where $\mathbf{C}_{CT}$ is the $N_C \times N_T$ matrix of tyre compliances at the points in the contact patch. These compliances can be calculated as a subset of the mobilities in Eq. (3), divided by $\mathrm{j}\omega$.

The vector of radial velocities for the tyre due to the road roughness can then be calculated from Eqs. (3)–(5), as

$$\mathbf{v}_T = \mathbf{T}\mathbf{d}, \tag{6}$$

where the overall transfer matrix, $\mathbf{T}$, is equal to $\mathbf{Y}_F[\mathbf{I} + \mathbf{K}_{TC}\mathbf{C}_{CT}]^{-1}\mathbf{K}_{TC}$.

2.3. The road excitation

Robson [18] described the excitation of a vehicle while travelling over a road surface by means of the concept of random process theory. He proposed a road surface classification method based on a single direct spectral density function of the road roughness. The statistical properties of the road surface displacement can be described by its spatial correlation function or its wavenumber spectrum, which Robson suggests falls off in approximate inverse proportional to the square of the wavenumber. This author also discusses experimental evidence for the roughness being approximately homogeneous and isotropic and he propose a two-dimensional Gaussian model. The ISO 8608 standard [19] also suggests using a similar description of the road profile.

The excitation of the tyre as it runs over a rough road is modelled as a random displacement distribution with a specified spatial correlation. If the contact patch is divided into a fine grid, the force distribution can be approximated by a vector of forces acting at the elements defined by the grid. Each force will have a random time history, which we will assume to be stationary, with its own autocorrelation function and a set of cross-correlation functions with the other forces acting in the contact patch. This spatial correlation partly arises because the road surface roughness will have a distribution of lengthscales and the larger peaks will be in contact with the tyre over a significant distance.

The road roughness is a random variable whose properties vary with the type of road surface, as described by Robson [18]. The time varying road displacement $d(t)$ is derived from traversing, at velocity v, a rigid road profile. The excitation spectral density $S_d(f)$ at a contact point can be derived for any particular vehicle velocity as

$$S_d(f) = \frac{c}{v}\left(\frac{f}{v}\right)^{-2.5}, \tag{7}$$

where f is the excitation frequency and c is a constant given in Ref. [18].

In the frequency range of interest, i.e. 10–400 Hz, and considering a range of velocities between 20 and 100 km/h, we require a road roughness valid for wavelength between 1 mm and 3 m, as shown in Fig. 3. However, the tyre elements in the contact area have a width of 2.3 mm, so the model can be considered reliable only up to excitation wavelength of about 5 mm in order to avoid geometric aliasing. Although the roughness road spectral description using Eq. (7) was originally proposed in Ref. [18] for wavelengths between 100 mm and 1 km, the model has been assumed to be valid over the range of wavelengths of interest here [20,21].

For a vehicle travelling at a constant velocity, the imposed displacement may be considered as a realisation of a multi-variate stationary random process and so may be described by a spectral density matrix. Each contact point travels over the same profile as that of the forward contact points, so that each point experiences, after a speed-dependent delay, the same imposed displacement.

A frequency-domain formulation will be used so that each displacement variable corresponds to the Fourier transform of a long time history, although the explicit dependence on frequency, ω, will be suppressed for notational convenience. The individual complex displacements are grouped together in an $N_C \times 1$ vector, **d**,

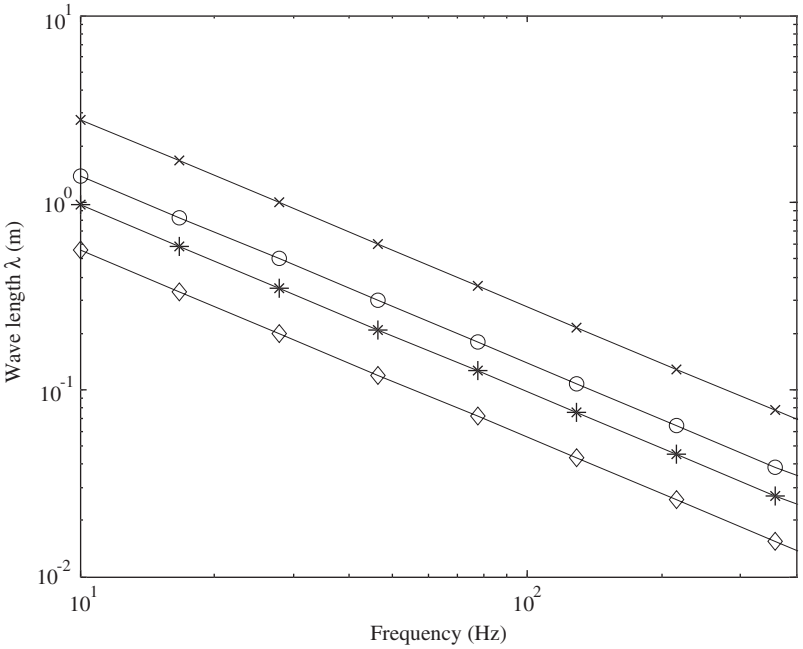

Fig. 3. Relationship between road roughness wavelength and frequency for speeds of: ◇ 20 km/h, ∗ 35 km/h, ○ 50 km/h, × 100 km/h.

and the spectral density matrix of the road displacement is then defined to be

$$\mathbf{S}_{dd} = \mathrm{E}[\mathbf{d}\mathbf{d}^{\mathrm{H}}], \tag{8}$$

where E denotes the expectation operator and $(\cdot)^{\mathrm{H}}$ denotes the Hermitian, complex conjugate, transpose. The diagonal elements of $\mathbf{S}_{dd}$ correspond to the power spectral densities of each of the displacements, which will be assumed to be equal in this model, and the off-diagonal terms correspond to cross spectral densities between the displacement at different points.

3. Tyre–road excitation results

If the models of the tyre, of the contact and of the road excitation are put together, a fully linear model can be obtained and random vibration analysis theory applied. The spectral density matrix of the tyre's elemental velocities, $\mathbf{S}_{vv}$, due to the road excitation can be expressed, using Eq. (6), in terms of the spectral density matrix of road displacement, $\mathbf{S}_{dd}$ in Eq. (8), as

$$\mathbf{S}_{vv} = \mathbf{T}\mathbf{S}_{dd}\mathbf{T}^{\mathrm{H}}. \tag{9}$$

Eq. (9) demonstrates the simplicity of the proposed analysis method, i.e. it is possible to express in just one equation the relationship between road profile and tyre vibration. The force transmitted to the hub of the tyre can also be calculated, as well as the noise radiated by the tyre given the tyre acoustical impedance matrix. The structure-borne sound inside the vehicle could be calculated from the tyre's mechanical impedance matrix, from tyre velocities to hub forces, and the vehicle's acoustic impedance matrix, from hub forces to internal pressures.

More simply, the model allows the calculation of the kinetic energy of the tyre associated with the motion of the tyre travelling over a rough road at various road speeds. The expectation of the kinetic energy, E_k, can be calculated considering the mass normalised mode shape matrix, $\mathbf{\Psi}$, and it is given by

$$E_k(\mathrm{j}\omega) = \tfrac{1}{2}\mathrm{trace}\{\mathbf{\Psi}^{+}\mathbf{S}_{vv}\mathbf{\Psi}^{+\mathrm{H}}\}, \tag{10}$$

where $(\cdot)^{+}$ is the pseudo-inverse operator.

Fig. 4 shows the kinetic energy evaluated at different car speeds, for the tyre parameters listed in Table 1, which illustrates that as well as an overall increase in level, greater speeds also tends to emphasise the resonant

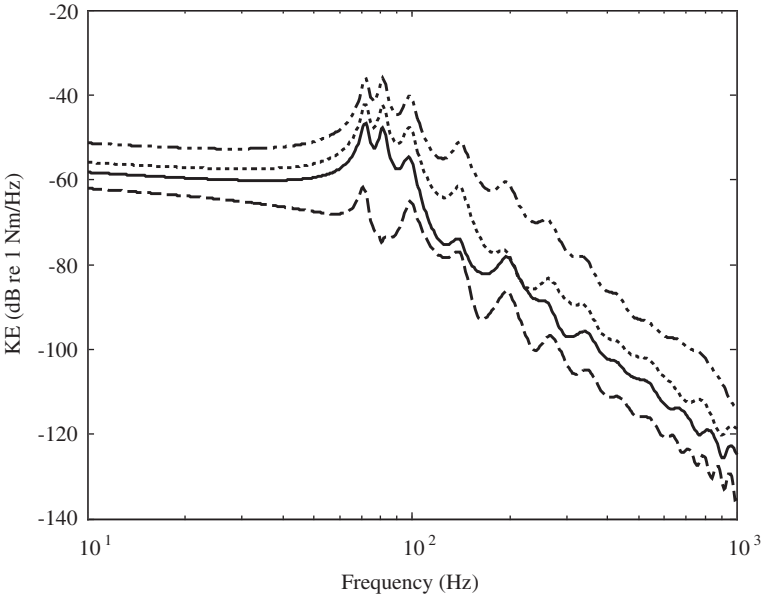

Fig. 4. Expected value of the kinetic energy, shown in the form of power spectrum density, evaluated at different car speeds: – · · – 100 km/h; · · · 50 km/h; —— 35 km/h; – – – 20 km/h.

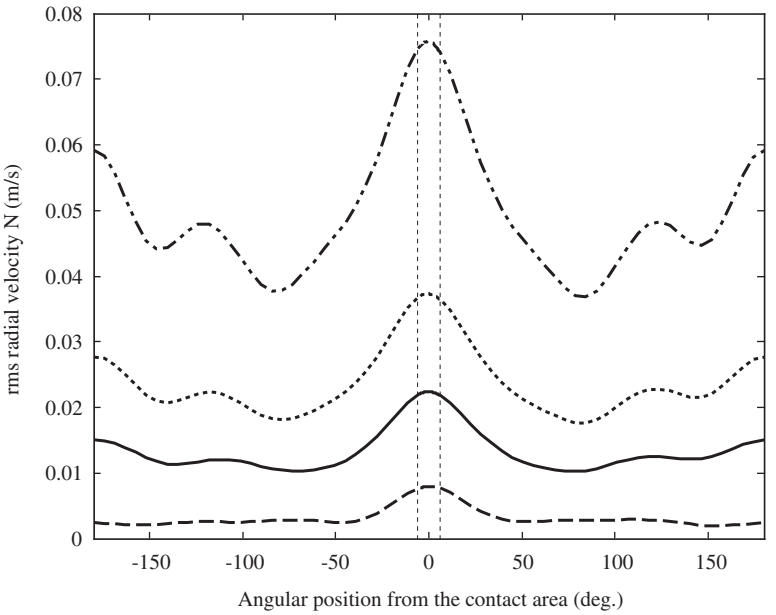

Fig. 5. Root mean square of the tyre element radial velocity, evaluated at different car speeds: – · · – 100 km/h; · · · 50 km/h; —— 35 km/h; – – – 20 km/h. The dashed vertical lines denote the extent of the contact patch.

response at about 100 Hz. The evaluated kinetic energy fall off of about 60 dB in the frequency range of interest and this is comparable with the experimental results reported in Ref. [22].

Fig. 5 shows the predicted radial rms velocity distribution around the tyre, calculated from the diagonal elements of $\mathbf{S}_{vv}$ in Eq. (9). As expected, the tyre velocity at the contact patch is much larger than in the rest of the tyre, and the velocity falls off away from the contact patch, because of the high damping of the rubber material. In the same way it is possible to calculate the expected radial acceleration, and this can be compared with the experimental results obtained by placing an accelerometer on the interior surface of a tyre [22,23] in order to measure the radial acceleration of the tyre tread. The acceleration measured in the experimental tests is partly due to the road excitation and partly due to the deformation of the tyre during rotation caused by the static loading of the car. The predicted acceleration is of the same order of magnitude, although a little lower, than the acceleration measured in Refs. [22,23], away from the contact patch, giving further support to the reliability of the model.

If the hub is divided into the same number of elements as the tyre, the force acting on each element of the hub is directly related to the displacement of the corresponding tread element by the sidewall stiffness. By integration over the circumference, the power spectrum matrix of the total force acting on the hub is

$$\mathbf{S}_{FF} = -\frac{1}{\omega^2}\mathbf{\Gamma}\mathbf{\Lambda}\mathbf{S}_{vv}\mathbf{\Lambda}^{\mathrm{H}}\mathbf{\Gamma}^{\mathrm{H}}, \tag{11}$$

where $\mathbf{\Gamma}$ is the transfer matrix from radial and tangential elemental forces to the horizontal and vertical global forces and $\mathbf{\Lambda}$ is the global sidewall stiffness matrix.

Fig. 6 shows the calculated force transmitted to the hub. The vertical force has a root mean value that varies from 2.44 to 15.09 N whereas the horizontal one varies from 0.17 to 0.37 N, as the speed of the car changes from 20 km/h to 100 km/h. Such forces are only due to the dynamical excitation and not to the static load. The vertical forces are in reasonable agreement with the experimental results reported in Ref. [24]. The horizontal forces are much smaller than the real case, however, since the tyre rotation and the contact friction have not been considered.

4. Control implementation

The case in which an additional set of controllable forces act on the tyre to implement active control is now considered. The key assumptions in this analysis is that the system is linear so that superposition can be

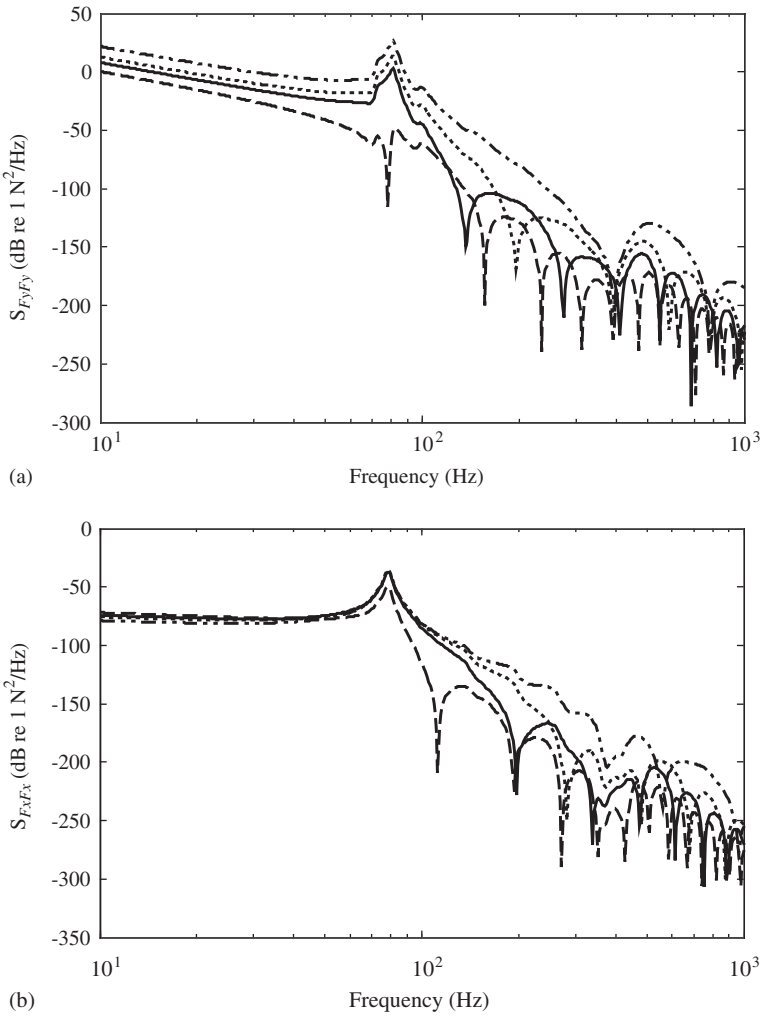

Fig. 6. Expected value of the force transmitted to the rigid hub, shown in the form of power spectrum density for the vertical (a) and horizontal (b) components, evaluated at different car speeds: – · · – 100 km/h; · · · 50 km/h; —— 35 km/h; – – – 20 km/h.

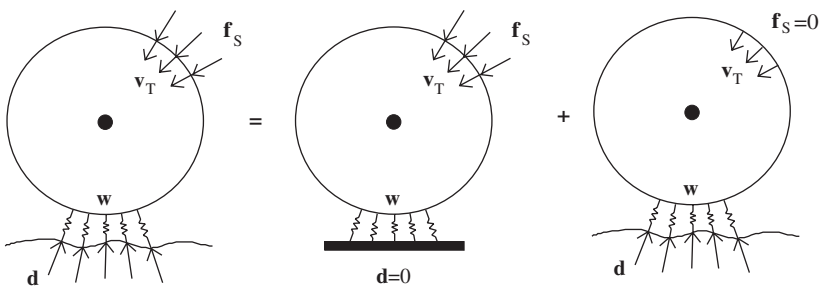

Fig. 7. Superposition effect of the controller.

applied as shown in Fig. 7. Then Eq. (6) becomes

$$\mathbf{v}_T = \mathbf{T}\mathbf{d} + \mathbf{Y}\mathbf{f}_S, \tag{12}$$

where $\mathbf{f}_S$ is the vector of N_S secondary forces that act on the tyre resting on the road surface and $\mathbf{Y}$ is overall mobility from the secondary excitation to the velocity vector that is given by $\mathbf{Y} = \mathbf{Y}_F[\mathbf{I} + \mathbf{K}_{TC}\mathbf{C}_{CT}]^{-1}\mathbf{T}_S$, where

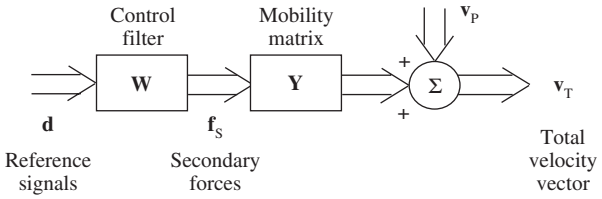

Fig. 8. Block diagram for the active control formulation. The broad arrows represent vector signals.

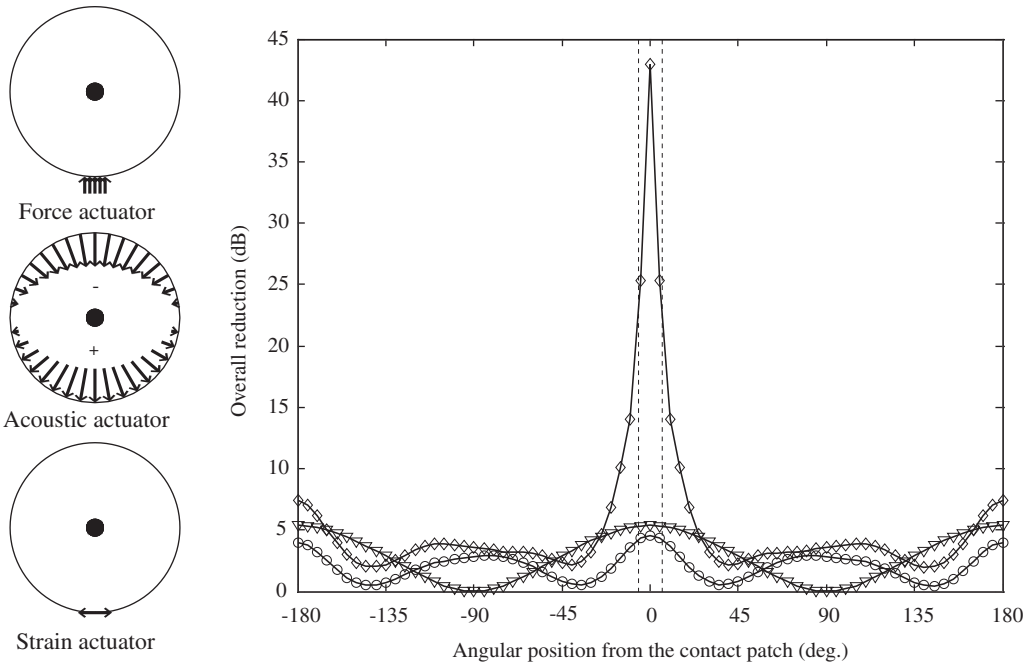

Fig. 9. Influence of the position of the actuator on the reduction of the global kinetic energy at 80 km/h: ◇ force actuator, ▽ acoustic actuator, ◯ strain actuator.

$\mathbf{T}_S$ is an $N_T \times N_S$ matrix that defines how each secondary force acts on the grid of elements we have chosen for the tyre. The block diagram for this arrangement is shown in Fig. 8 where the broad arrows represent vector signals.

In order to determine the physical limits of control with various secondary actuators, a feedforward control strategy is assumed, with perfect knowledge of the forces in the contact patch. For simplicity, the analysis is performed in the frequency domain without the constraint of causality. The secondary forces are assumed to be driven from a set reference signals equal to the road displacements, **d**. These reference signals are passed through a matrix of filters with frequency response **W** so that $\mathbf{f}_S = \mathbf{W}\mathbf{d}$.

The matrix of control filters, **W**, which minimises a quadratic cost function of the form given by Eq. (10) is then [25]

$$\mathbf{W}_{\text{opt}} = -[\mathbf{Y}^{\text{H}}\mathbf{Q}\mathbf{Y}]^{-1}\mathbf{Y}^{\text{H}}\mathbf{Q}\mathbf{T}, \tag{13}$$

where $\mathbf{Q} = \frac{1}{2}\mathbf{\Psi}^{+\text{H}}\mathbf{\Psi}^{+}$ in this case.

Attention has been focused on modelling different kinds of potential actuators to be used individually. Three different kinds of actuators have been considered: a distributed force actuator, that might be implemented with an electromagnet for example, a strain actuator, that might be implemented with a piezo-ceramic device for example, and an acoustic actuator, that might be implemented with a pair of loudspeakers inside the tyre exciting the first acoustic mode. Fig. 9 illustrates the assumed force distribution generated by

these actuators. The force actuator exerts a radial force at the tread whereas the strain actuator generates a pair of tangential forces at the tread. The acoustic actuator exerts a pressure around the tyre with a sinusoidal distribution corresponding to the first acoustic mode of the tyre interior, so that it couples into the vertical displacements of the tyre. The attenuation in the global kinetic energy, integrated up to 1 kHz, that can be obtained for each of these actuators with the optimal controller given in Eq. (13) has been computed and Fig. 9 shows how this reduction, for a car speed of 80 km/h, varies with the angular position at which the actuator is placed. The contact patch extends from an angular position of $\pm 5.8^{\circ}$ in this model, since the contact length is about 7 cm.

It is clear that a potentially large reduction can be obtained in the kinetic energy using a force actuator placed nearby the contact patch. Away from the contact patch the performance of the different actuators are very similar. Even the acoustic actuator that acts on the most relevant mode shape does not have a such great effect as the force actuator. Hence, it can be inferred that in order to reduce tyre vibration generated by the road interaction it is much more important to counteract the excitation than to try to reduce the resultant tyre vibrations.

Such results demonstrate the utility and efficiency of the analysis method outlined in Section 2. The active control results, however, are very preliminary and idealised and there is a long way to go before practical actuators are developed for this application and such a methodology can be validated and applied to the real case.

5. Conclusions

A ring model for the tyre and a linear contact model have been used to describe the behaviour due to tyre/road interactions. This linear model can be used to calculate the kinetic energy of the tyre due to both road excitation, specified by the spectral density matrix of a set of road displacements, and to a set of controllable secondary force distributions. Such a two-dimensional ring model allows the low-frequency response (up to about 400 Hz) of the tyre to a rough road to be calculated in a straightforward way for various road speeds, although the current model does not account for rotation of the tyre, in common with several other models to be found in the literature. The method presented in this paper can give a simple and intuitive prediction of the low-frequency tyre tread velocity and hence also of sound radiation. The predicted results are in reasonable agreement with the measured results that are available. Although a more complete model would need to include the nonlinear interaction in the contact patch and the effects of tyre rotation, the present formulation appears to give a reasonable first-order description of tyre interaction. A further study is current underway to develop a fully nonlinear contact model and this will be the subject of a future publication. A feedforward control formulation has then been used to estimate the attenuation in the response of the tyre on a particular road surface with particular types of secondary actuator. Useful reductions are predicted for a force actuator acting close to the contact patch, although many practical problems need to be overcome before such active systems could be implemented in practice.

Acknowledgments

The work of E. Rustighi is supported by the EU under the integrated project "Integrated materials for active noise reduction", InMAR. We are pleased to acknowledge the helpful advices of Dr. S. Finnveden.

References

[1] U. Sandberg, Tyre/road noise—myths and realities, *Proceedings of Inter-Noise 2001*, 2001, pp. 35–56.

[2] U. Sandberg, G. Descornet, Road surface influence on tyre/road noise—part i, *Proceedings of Inter-Noise 80*, Vol. 1, 1980, pp. 259–266.

[3] S. Jha, Identification of road/tyre induced noise transmission paths in a vehicle, *International Journal of Vehicle Design* 5 (1/2) (1984) 143–158.

[4] A. Kuijpers, G. van Blokland, Tyre/road noise models in the last two decades: a critical evaluation, *Proceedings of Inter-Noise 2001*, The Hague, The Netherlands, 2001, pp. 2593–2598.

[5] W. Kropp, F.-X. Bécot, S. Barrelet, On the sound radiation from tyres, *Acoustica* 86 (2000) 760–779.
[6] S. Fong, Tyre induced predictions from computed road surface texture induced contact pressure, *Internoise 98*, Christchurch New Zealand, 1998.
[7] W. Kropp, Structure-borne sound on a smooth tyre, *Applied Acoustics* 26 (1989) 181–192.
[8] K. Larsson, W. Kropp, A high frequency three-dimensional tyre model based on two coupled elastic layers, *Journal of Sound and Vibration* 253 (4) (2002) 889–908.
[9] R.J. Pinnington, A.R. Briscoe, A wave model for a pneumatic tyre belt, *Journal of Sound and Vibration* 253 (5) (2002) 941–959.
[10] J.M. Muggleton, B.R. Mace, M.J. Brennan, Vibrational response prediction of a pneumatic tyre using an orthotropic two-plate wave model, *Journal of Sound and Vibration* 264 (4) (2003) 929–950.
[11] T.G. Clapp, A.C. Eberhardt, C.T. Kelley, Development and validation of a method for approximating road surface texture-induced contact pressure in tire-pavement interaction, *Tire Science and Technology* 16 (1) (1988) 2–17.
[12] F. Wullens, W. Kropp, A three-dimensional contact model for tyre/road interaction in rolling conditions, *Acta Acoustica United with Acoustica* 90 (2004) 702–711.
[13] S. Huang, W. Soedel, Effects of coriolis acceleration on the free and forced in-plane vibrations of rotating rings on elastic foundation, *Journal of Sound and Vibration* 115 (2) (1987) 253–274.
[14] L.E. Kung, W. Soedel, T.Y. Yang, Free vibration of a pneumatic tyre-wheel unit using a ring on an elastic foundation and a finite element model, *Journal of Sound and Vibration* 107 (2) (1986) 181–194.
[15] Y.-J. Kim, J.S. Bolton, Effects of rotation on the dynamics of a circular cylindrical shell with application to tire vibration, *Journal of Sound and Vibration* 275 (2004) 605–621.
[16] K. Johnson, *Contact Mechanics*, Cambridge University Press, Cambridge, 1985.
[17] K. Larsson, Modelling of Dynamic Contact—Exemplified on the Tyre/Road Interaction, PhD Thesis, Department of Applied Acoustics, Chalmers University of Technology, Göteborg, Sweden, 2002.
[18] J. Robson, Road surface description and vehicle response, *International Journal of Vehicle Design* 1 (1) (1979) 25–35.
[19] Mechanical vibration—road surface profiles—reporting of measured data, ISO 8608, 1995.
[20] U. Sandberg, Road traffic noise—the influence of the road surface and its characterization, *Applied Acoustics* 21 (1987) 97–118.
[21] P. Andersson, Modelling Interfacial Details in Tyre/Road forces Contact—Adhesion Forces and Non-linear Contact Stiffness, PhD Thesis, KTH, Chalmers University of Technology, Göteborg, Sweden, 2005.
[22] J. Périsse, A study of radial vibrations of a rolling tyre for tyre-road noise characterisation, *Mechanical Systems and Signal Processing* 16 (6) (2002) 1043–1058.
[23] W. Kropp, K. Larsson, F. Wullens, P. Andersson, Tyre/road noise generation, *Proceedings of the Institute of Acoustics* 26 (2) (2004) 1–12.
[24] M. Minakawa, J. Nakahara, J. Ninomiya, Y. Orimoto, Method for measuring force transmitted from road surface to tires and its applications, *JSAE Review* 20 (1999) 479–485.
[25] S. Elliott, *Signal Processing for Active Control*, Academic Press, New York, 2001.